Investigation on the Luminescence Improvement of Nanosized La2O3/Eu3+ Phosphor under Charge-Transfer Excitation

ARTICLE *in* THE JOURNAL OF PHYSICAL CHEMISTRY C · JANUARY 2011

Impact Factor: 4.77 · DOI: 10.1021/jp108608f

THE JOURNAL OF PHYSICAL CHEMISTRY C

ARTICLE

pubs.acs.org/JPCC

Investigation on the Luminescence Improvement of Nanosized La_2O_3/Eu^{3+} Phosphor under Charge-Transfer Excitation

Chunyu Shang,*[,†,‡] Hongbo Jiang,[‡] Xiaohong Shang,[§] Meicheng Li,[†] and Liancheng Zhao[†]

[†]Department of Information Materials Science and Technology, School of Materials Science and Engineering, Harbin Institute of Technology, Harbin 150001, China

[‡]Automatic Engineering Department, Heilongjiang Institute of Science and Technology, Harbin 150027, China

[§]School of Chemistry and Life Science, Changchun University of Technology, Changchun 130052, China

ABSTRACT: When the size of La_2O_3/Eu^{3+} phosphor decreases to the nanoscale, the rigidity of the lattice environment is decreased, causing the enlargement of the charge-transfer state (CTS) coordinate offset for the optical centers in La_2O_3/Eu^{3+} nanophosphor. The enlargement of the CTS coordinate offset results in the decrease of the CTS feeding probability to the ^5D states of Eu^{3+} ions in the optical centers. In addition, the energy transfer to the quenching centers in the surface leads to the decrease of the ^5D emission efficiency of the excited Eu^{3+} ions. In view of these two quenching mechanisms of the optical centers, proper surface coating is adopted to improve the luminescence efficiency for La_2O_3/Eu^{3+} nanophosphor under CT excitation. The changes in the related parameters of La_2O_3/Eu^{3+} nanophosphor in the surface coating and the subsequent annealing process have been experimentally determined and objectively analyzed. By surface coating, the luminescence efficiency of La_2O_3/Eu^{3+} nanophosphor has been significantly improved.

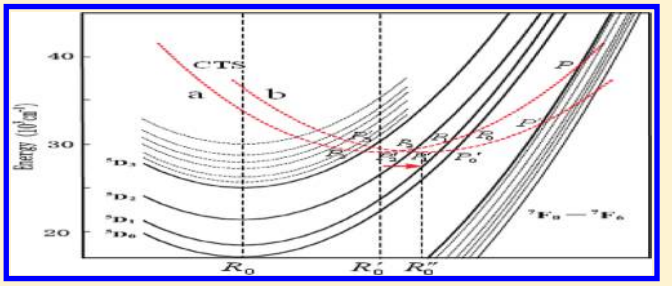

1. INTRODUCTION

When the size of many kinds of luminescent materials decreases to the nanoscale, the surface effects become apparent. The nanosized luminescent materials exhibit a series of novel structural, electronic, and optical properties which are not present in the corresponding bulk materials.[1] The advances made in the size reduction of optical devices require sufficient understanding of the physical properties of luminescent materials with size on the nanoscale.[2] It is expected that high-resolution images may be achieved with nanosized luminescent materials.[3] As a kind of very important surface effect, the decrease of luminescence efficiency becomes apparent with the size decrease in the nanoscale for many kinds of luminescent materials. In order to ensure the applicability of nanosized luminescent materials, the techniques improving the luminescence efficiency should be investigated. In principle, the specific techniques should be based on the specific mechanisms causing the decrease of luminescence efficiency for a specific kind of luminescent material. However, for different kinds of luminescent materials and different types of excitation, the reasons influencing the luminescence efficiency should be different and complex. As an important type of red-emitting luminescent material, Eu^{3+}-doped phosphors can be excited by charge transfer (CT) excitation. They are very popular and extensively applied in fluorescent lighting and display.[4−6] In this paper, by taking La_2O_3/Eu^{3+} nanophosphor as the investigating object, the mechanisms influencing the luminescence efficiency for Eu^{3+}-doped nanophosphors have been typically investigated. In view of the quenching mechanisms of the optical centers in La_2O_3/Eu^{3+} nanophosphor, a proper surface coating is adopted to improve the luminescence efficiency. The changes in the related parameters of La_2O_3/Eu^{3+} nanophosphor in the surface coating have been experimentally determined, and higher luminescence efficiency has been achieved.

2. EXPERIMENTAL SECTION

A nanosized La_2O_3/Eu^{3+} ($(La_{0.97}Eu_{0.03})_2O_3$) sample was prepared by glycine nitrate solution combustion synthesis.[7,8] In brief, analytical-grade lanthanide nitrate ($La(NO_3)_3\cdot 6H_2O$, $Eu(NO_3)_3\cdot 6H_2O$) and glycine ($C_2H_5NO_2$) were dissolved (glycine-to-nitrate molar ratio of 1.9:1) in distilled water to form the precursor solution. The precursor solution was concentrated by heating at 240 °C until spontaneous combustion occurred and the La_2O_3/Eu^{3+} sample was formed. The La_2O_3/Eu^{3+} sample was then annealed at 500 °C for 1 h to be purified. On the basis of the XRD data and Scherrer's equation, the size of the La_2O_3/Eu^{3+} sample was determined to be about 30 nm. The bulk

Received: September 9, 2010
Revised: December 26, 2010
Published: January 24, 2011

La_2O_3/Eu^{3+} sample was obtained by sintering the nanosized La_2O_3/Eu^{3+} sample at 1250 °C for 3 h.

The nanosized La_2O_3/Eu^{3+} sample was coated with SiO_2 by the Stöber method;[9,10] 1.0 g of the nanosized La_2O_3/Eu^{3+} sample was added into 200 mL of isopropyl alcohol ($(CH_3)_2$-CHOH) to form the suspension. The suspension was stirred with ultrasonic oscillation for 30 min to disperse the particles; then, 30 mL of deionized water and 20 mL of hydrous ammonia ($CH_3 \cdot H_2O$) were added, and 10 min later, 1.24 mL of tetraethyl orthosilicate (TEOS) was gradually dropped into the suspension under stirring. After adequate reaction, the product was taken out by centrifuging and rinsed twice in deionized water. The reaction product was heated at 200 °C for 2 h to form the SiO_2-coated La_2O_3/Eu^{3+} sample (the weight ratio of La_2O_3/Eu^{3+} to SiO_2 is 3:1). The sample was then annealed at 800 °C for 1 h to form the SiO_2-coated and annealed La_2O_3/Eu^{3+} sample.

The crystalline phases of the nanosized La_2O_3/Eu^{3+} samples were identified by Rigaku-D/max 2500 X-ray diffractometer using Cu Kα radiation (λ = 0.15405 nm). The morphology of the core−shell structure of the SiO_2-coated La_2O_3/Eu^{3+} sample was characterized using a JEOL-1010 transmission electron microscope. Fourier transform infrared spectra (FT-IR) were measured using a Varian 800 FT-IR Scimitar Series spectrometer with the potassium bromide (KBr) pellet technique. Under the excitation of the fourth-frequency pulse of a Nd:YAG laser at 280 nm, the luminescence decay curves of the La_2O_3/Eu^{3+} samples were recorded by monitoring the output of a R456 photomultiplier tube with a Tektronic TDS 3052 digital oscilloscope. The measurement of the CT emission spectra for the nanosized La_2O_3/Eu^{3+} samples was performed with an FLS 920 fluorescence spectrometer equipped with a 150 W xenon lamp as the excitation source. All of the measurements were performed at room temperature.

3. RESULTS AND DISCUSSION

3.1. Enlargement of the CTS Coordinate Offset in CCD for Nanosized La_2O_3/Eu^{3+} Phosphor. For the CT excitation of La_2O_3/Eu^{3+} phosphor, the optical center is composed of a central Eu^{3+} ion binding with its ligand O^{2-} ion. In the breathing model of the optical center, the ligand pulsates in and away from the central ion, and a harmonic oscillator mode can describe the pulsations. The energy of the optical center, including the vibrational energy of the ligand, is depicted by parabolas in the configurational coordinate diagram (CCD).[11] There are a series of parallel parabolas labeled $^7F_0, ^7F_1, \ldots$; $^5D_0, ^5D_1, ^5D_2, ^5D_3, \ldots$ in the CCD, denoting the energy states of the optical center when the central Eu^{3+} ion is in its different $4f^6$ levels. In CT excitation, an electron is transferred from the ligand O^{2-} ion to the central Eu^{3+} ion, and the optical center is in the CT state (CTS) when the central Eu^{2+} ion is in the ground state $^8S_{7/2}$. The charge transfer causes the relaxation of the equilibrium distance between the central Eu^{2+} ion and its ligand O^- ion from R_0 to a larger value R_0', and the optical center is expanded.[12] It has been reported that the ionic radius of the Eu^{2+} ion is 18 pm larger than that of the Eu^{3+} ion; this is a second factor that contributes to the relaxation of the equilibrium distance or the expansion of the optical center.[12] Because the optical center is incorporated in the host lattice, unavoidably, its expansion would be restricted by the lattice, and the expanding degree should be determined by the rigidity of the lattice environment in which the optical center is located. When the lattice is softer, the expansion of the optical center, that is, the CTS coordinate offset $R_0' - R_0$, would be larger.

Table 1. Related Parameters Measured or Calculated for (S_1) Bulk, (S_2) 30 nm, (S_3) 30 nm SiO_2-Coated, and (S_4) 30 nm SiO_2-Coated and Annealed La_2O_3/Eu^{3+} Samples

samples	R	A_R (s^{-1})	τ (ms)	η	$\int_{0-2} I(\nu)\, d\nu$	ratio of $P_{CTS,D}$
S_1	10.46	414.43	2.07	0.8579	1.061×10^7	1
S_2	11.52	456.42	1.27	0.5797	3.623×10^6	0.505
S_3	11.45	453.65	1.35	0.6124	5.297×10^6	0.699
S_4	11.20	443.74	1.67	0.7410	8.323×10^6	0.908

It has been reported that the resistance effect of amorphous phosphors to the expansion of an excited optical center is weaker than that of crystal phosphors, and the CTS coordinate offset is larger in amorphous phosphors than that in homogeneous crystal phosphors.[13] For instance, the CTS coordinate offset is larger in amorphous SrB_4O_7/Eu^{3+} phosphor than that in crystalline SrB_4O_7/Eu^{3+} phosphor, leading to the enlargement of the Stokes shift ($2S\hbar\omega$) of amorphous SrB_4O_7/Eu^{3+} phosphor ($S\hbar\omega = (1/2)K(R_0' - R_0)^2$).[13] Because of the enlargement of the CTS coordinate offset, the magnitude of the luminescence efficiency for Eu^{3+}-doped amorphous phosphors is smaller than that of homogeneous crystal phosphors, leading to the decrease of quenching temperature for Eu^{3+}-doped amphorous phosphors.[14] In fact, the enlargement of the CTS coordinate offset in amorphous phosphors can be explained easily from the local disorder of chemical bonds and atom arrangement around the optical centers. There has been much research work on the local structure of nanophosphors, revealing that the local structure obviously changes and becomes more complicated when the phosphor size decreases to the nanoscale.[1,15] In particular, for Eu^{3+}-doped phosphors, the ratio of the integrate intensities of the $^5D_0 \rightarrow {}^7F_2$ hypersensitive electric dipole transition to the $^5D_0 \rightarrow {}^7F_1$ magnetic dipole transition

$$R = \frac{I(^5D_0 \rightarrow {}^7F_2)}{I(^5D_0 \rightarrow {}^7F_1)} \quad (1)$$

is considered indicative of the asymmetry of the local environment around the Eu^{3+} ions. R is called the asymmetry ratio; for a certain kind of Eu^{3+}-doped phosphor, a larger value of R means a larger local disorder of the lattice environment.[16] In our experiments, the asymmetry ratio R of bulk and nanosized La_2O_3/Eu^{3+} samples has been calculated and is listed in Table 1. It is apparent that the local disorder is enlarged when the size of La_2O_3/Eu^{3+} phosphor decreases to the nanoscale (different R for S_1 and S_2), and the structure tends to be amorphous. It is therefore concluded that the CTS coordinate offset would become larger when the size of La_2O_3/Eu^{3+} phosphor decreases to the nanoscale.

There is a second important reason that contributes to the enlargement of the CTS coordinate offset for La_2O_3/Eu^{3+} nanophosphor. When the phosphor size decreases to the nanoscale, the surface-to-volume ratio increases greatly, and there will be relatively more optical centers near the surface. When an optical center is nearer the surface, the atomic layer between the optical center and the surface is thinner, and there will be fewer atoms and fewer chemical bonds that participate in the resistance to the expansion of the excited optical center, and the rigidity of the lattice environment around the optical center is further

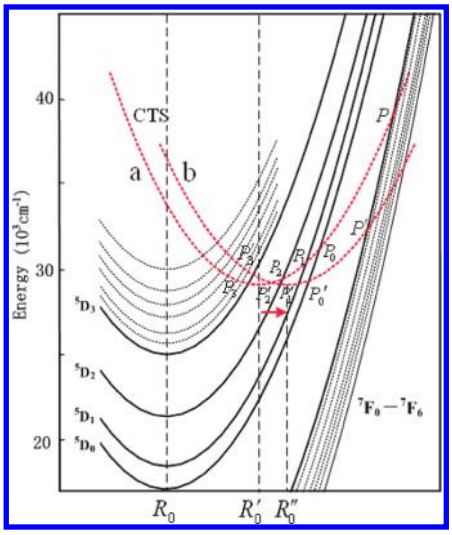

Figure 1. The right shift of the CTS parabola in CCD for nanosized La_2O_3/Eu^{3+} phosphor. Parabolas a and b represent the CTS for bulk and nanosized La_2O_3/Eu^{3+} phosphors, respectively.

decreased. Consequently, the enlargement of the CTS coordinate offset becomes more apparent.

Assuming that the rigidity of the lattice environment in La_2O_3/Eu^{3+} nanophosphor is of the same magnitude as that of ordinary amorphous phosphors, then the relative enlargement $(R_0'' - R_0')/(R_0' - R_0)$ of the CTS coordinate offset can be evaluated to be less than 10%.[14] The enlargement of the CTS coordinate offset means the right shift of the CTS parabola in CCD, as illustrated by the arrow in Figure 1.

3.2. Mechanism for the Decrease of the CTS Feeding Probability to the ^5D States for La_2O_3/Eu^{3+} Nanophosphor. As has been pointed out above, the enlargement of the CTS coordinate offset means the right shift of the CTS parabola in CCD. The right shift of the CTS parabola in CCD leads to the shift of the crossovers p_J between the CTS and the ^5D_J states ($p_0 \rightarrow p_0'$, $p_1 \rightarrow p_1'$, $p_2 \rightarrow p_2'$, $p_3 \rightarrow p_3'$), and the crossover for a lower ^5D state is decreased relative to the crossover for a higher ^5D state (see Figure 1).

In the CT excitation of an optical center, the optical center reaches the CTS. Subsequently, the CTS may feed the ^5D states of the Eu^{3+} ion through thermal transition; this process leads to the populations of the ^5D states, and the transition rate to each ^5D_J state is directly related to $E_{CTS,J}$ by the following formula[17]

$$K_{CTS,J} = A \exp\left(-\frac{E_{CTS,J}}{KT}\right) \quad (2)$$

where $E_{CTS,J}$ is the thermal barrier between the CTS and the ^5D state, that is, the height difference between the CTS minima and the crossover p_J in CCD.

For the $4f^6$ configuration of the Eu^{3+} ion, the ^7F levels are much lower than the ^5D levels, and this leads to the apparent height differences between the parallel ^7F and ^5D parabolas in CCD.[11] Contrasted with the transition from the CTS to the ^5D states, the transition from the CTS to the ^7F states means the quenching of the optical center. To compare the competition between the ^5D state and the ^7F state for the CTS transitions (for simplicity, the four ^5D_J states are represented by one ^5D state, and the seven ^7F_J states are represented by one ^7F state), the feeding probability from the CTS to the emitting ^5D state should be given as

$$P_{CTS,D} = \frac{A \exp\left(-\frac{E_{CTS,D}}{KT}\right)}{A \exp\left(-\frac{E_{CTS,D}}{KT}\right) + A \exp\left(-\frac{E_{CTS,F}}{KT}\right)} = \frac{1}{1 + \exp\left(-\frac{E_{P,P_0}}{KT}\right)} \quad (3)$$

where $E_{CTS,D}$ is the thermal barrier between the CTS and the ^5D state, $E_{CTS,F} = E_{CTS,D} + E_{P,P_0}$ is the thermal barrier between the CTS and ^7F state, and E_{P,P_0} is the height difference between the two crossovers p,p_0 in CCD.

When the size of La_2O_3/Eu^{3+} phosphor decreases to the nanoscale, the right shift of the CTS parabola in CCD leads to the decline of the crossover p relative to the crossover p_0, and E_{P,P_0} is decreased to $E_{P',P_0'}$($p_0 \rightarrow p_0'$,$p \rightarrow p'$). According to eq 3, the CTS feeding probability to the emitting ^5D state is decreased. Meanwhile, the transition probability from the CTS to the ^7F state is increased; the excitation of the optical center tends to be relaxed by sending phonons to the host lattice.

3.3. Utilization of Surface Coating to Improve the Luminescence Efficiency for La_2O_3/Eu^{3+} Nanophosphor. On the basis of the discussions above, we can see that the CTS feeding probability to the ^5D states is decreased for the optical centers in La_2O_3/Eu^{3+} nanophosphor due to the rigidity decrease of the lattice environment. On the other hand, as has been pointed out in the literature, with the decrease of phosphor size to the nanoscale, there will be relatively more quenching centers formed by the defects and dangling bonds in the surface, and the ^5D emission efficiency would be decreased due to the energy transfer from the excited Eu^{3+} ions to the quenching centers.[18−22] It is these two mechanisms that are playing key roles in the decrease of the luminescence efficiency for La_2O_3/Eu^{3+} nanophosphor under CT excitation. To know the reason is to know the solution; a proper surface coating method may be adopted to improve the luminescence efficiency of La_2O_3/Eu^{3+} nanophosphor. The suitable coating material should have the following proprieties: (1) high transparency in the wavelength regions of the excitation and emission light, (2) proper thickness of the coating layer, and (3) successful linkage between the phosphor and the coating material. The reasons for these requirements are obvious. Under proper surface coating, the rigidity of the lattice environment would be improved, and the CTS feeding probability to the ^5D states should be increased; the quenching centers (defects and dangling bonds) in the surface would be effectively eliminated, and the ^5D emission efficiency of the Eu^{3+} ions should be increased.

In our experiments, a nanosized La_2O_3/Eu^{3+} sample was coated with SiO_2 by the Stöber method; the weight ratio of La_2O_3/Eu^{3+} to SiO_2 was set to be 3:1, which was experimentally proven to be the proper ratio. The XRD results indicated that the SiO_2 layer remained amorphous after being annealed at 800 °C for 1 h. In order to confirm the formation of core−shell structure for the as-prepared sample, TEM measurements were performed. The core−shell structure can be observed clearly due to the different electron penetrability for the core and the shell, as shown in Figure 2. The FT-IR spectra for the La_2O_3/Eu^{3+} sample (a), SiO_2-coated La_2O_3/Eu^{3+} sample (b), and

SiO_2-coated and annealed La_2O_3/Eu^{3+} sample (c) are shown in Figure 3. In these three FT-IR spectra, the absorption bands of La−O (565 cm^{-1}), OH (3429 cm^{-1}), and H_2O (1630 cm^{-1}) are all observed, but the OH band is weaker in (c). It is well known that OH ions are a kind of quenching center for nanophosphors,[23] the quantity of which is decreased after the annealing of the SiO_2-coated La_2O_3/Eu^{3+} sample. In spectra (b) and (c), Si−O−Si (1118 cm^{-1}, 810 cm^{-1}) and Si−O (480 cm^{-1}) absorption bands are observed, but these two bands are stronger in spectrum (c), indicating that the structure of the SiO_2 layer has been improved by annealing. It has been reported that the Si−OH (954 cm^{-1}) groups play an important role in bonding with the metal ions (La^{3+}, Eu^{3+}) in the annealing process.[22] After the formation of a Si−O−La linkage, OH ions would be exhausted, the absorption band of which is diminished in spectrum (c).

After the surface coating and the subsequent annealing process, the structure of the SiO_2 layer is improved, and the core−shell linkage is strengthened. The atoms and chemical bonds in the SiO_2 layer will participate in the resistance to the expansion of the excited optical centers in the La_2O_3/Eu^{3+} phosphor; thus, the rigidity of the lattice environment around the optical centers is increased. In addition, the larger local disorder in La_2O_3/Eu^{3+} phosphor should be decreased in the surface coating and the subsequent annealing process (see the different R for S_2, S_3, and S_4 in Table 1), and the rigidity of La_2O_3/Eu^{3+} phosphor should be further increased in a certain extent. For these reasons, the CTS feeding probability to the ^5D states should be increased. On the other hand, the quantity of the quenching centers formed by the defects and dangling bonds in the surface should be significantly reduced due to the formation of the Si−O−La linkage. For this reason, the ^5D emission efficiency of the Eu^{3+} ions should be improved. After the surface coating and the subsequent annealing process, the luminescence efficiency of La_2O_3/Eu^{3+} phosphor should be necessarily improved.

The emission spectra for the noncoated, SiO_2-coated, and SiO_2-coated and annealed La_2O_3/Eu^{3+} samples are shown in Figure 4. On the basis of the integrated intensity measurements of the emission spectra under the same CT excitation conditions, the luminescence efficiency of the nanosized La_2O_3/Eu^{3+} sample is proven to be improved to about 1.5 times by surface coating

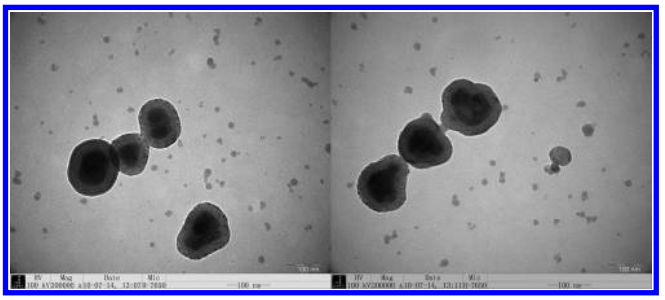

Figure 2. TEM micrographs for the SiO_2-coated La_2O_3/Eu^{3+} sample.

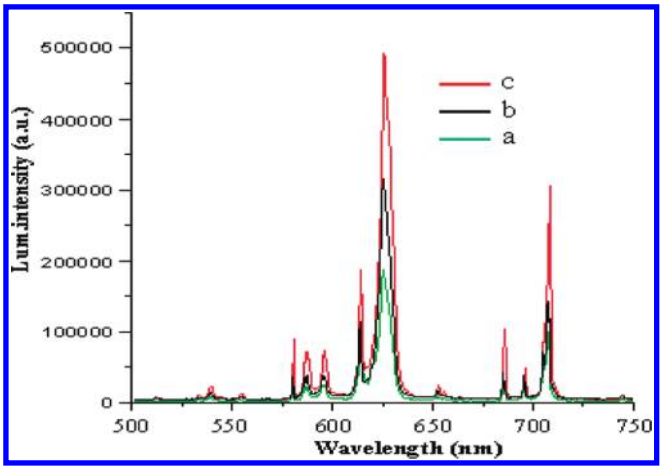

Figure 4. CT emission spectra for (a) 30 nm noncoated, (b) 30 nm SiO_2-coated, and (c) 30 nm SiO_2-coated and annealed La_2O_3/Eu^{3+} samples (excited by 280 nm UV light).

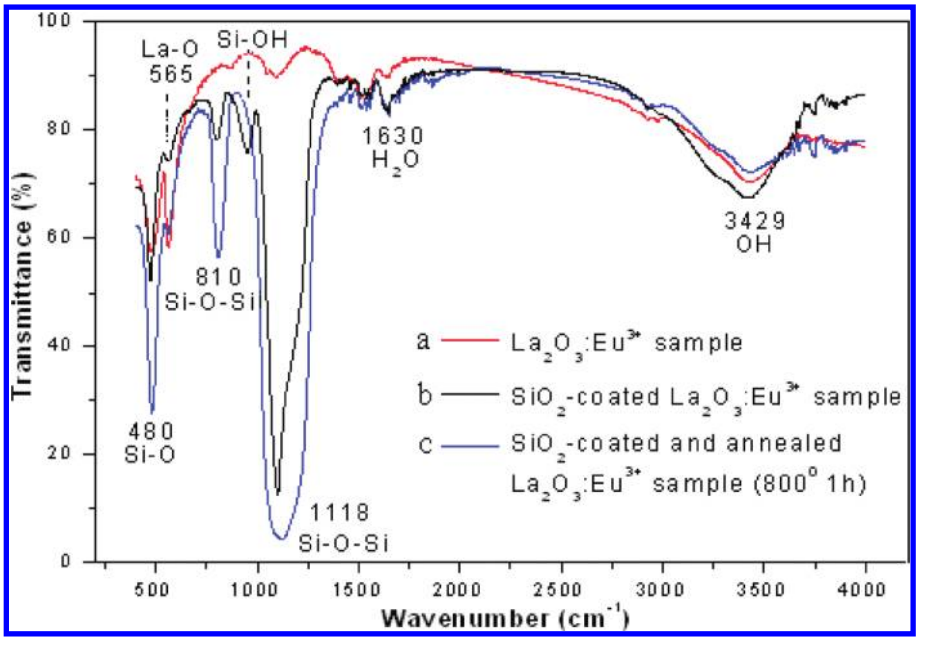

Figure 3. FT-IR spectra for (a) noncoated, (b) SiO_2-coated, and (c) SiO_2-coated and annealed La_2O_3/Eu^{3+} samples.

dx.doi.org/10.1021/jp108608f |J. Phys. Chem. C 2011, 115, 2630–2635

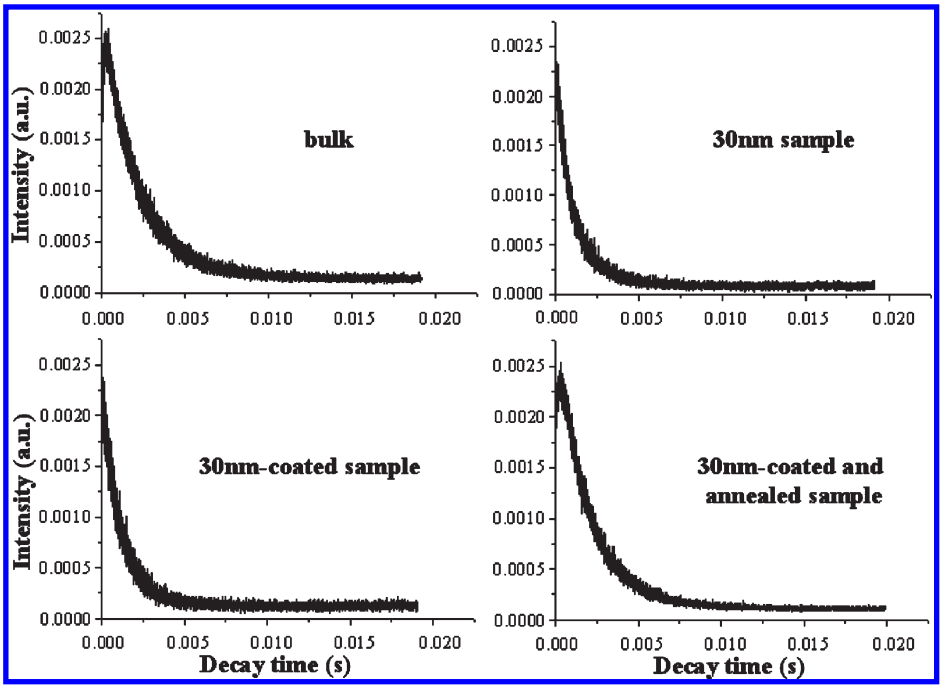

Figure 5. Luminescence decay curves of the La_2O_3/Eu^{3+} samples (λ_{ex} = 280 and 626 nm).

and is progressively improved to 2.3 times by surface coating and the subsequent annealing process.

3.4. Experimental Determination of the Related Parameters for the Different La_2O_3/Eu^{3+} Samples. In principle, the change in luminescence efficiency must originate from the changes in related parameters of the phosphor. Consequently, in order to get a clear understanding of the differences in luminescence efficiency for the La_2O_3/Eu^{3+} samples, the changes in the related parameters should be determined.

In the CT excitation of La_2O_3/Eu^{3+} phosphor, the CTS feeding leads to the population of Eu^{3+} ions in the ^5D states. Subsequently, the excited Eu^{3+} ions would relax to the $^5D_0$ state promptly through multiphonon relaxation. Consequently, the $^5D_0$ radiative transitions are dominant and representative in the emission spectra. Under CT excitation, the luminescence efficiency P of La_2O_3/Eu^{3+} nanophosphor is determined mainly by two parameters, (1) the CTS feeding probability $P_{CTS,D}$ to the ^5D states and (2) the $^5D_0$ emission efficiency η to the ^7F states. Their relation should be expressed as

$$P = A' \cdot P_{CTS,D} \cdot \eta \tag{4}$$

For the $^5D_0 \rightarrow {}^7F_1$ magnetic dipole transition, the radiation rate is determined by[24,25]

$$A_{md} = A_{0-1} = \frac{64\pi^4 \nu_{md}^3}{3h(2J+1)} n^3 S_{md} \tag{5}$$

where ν_{md} is the $^5D_0 \rightarrow {}^7F_1$ transition energy in wavenumbers, h is Plank's constant, 6.626×10^{-27}, n is the refractive index of the host lattice, $2J + 1$ is the degeneracy of the initial state (1 for $^5D_0$), and S_{md} is the oscillator strength of the magnetic dipole transition, which is independent of the host lattice, 7.83×10^{-42}.[26] For La_2O_3/Eu^{3+} phosphor, ν_{md} = 16950 cm^{-1}, n = 1.5, and A_{md} = 39.62 s^{-1}. The radiation rate A_R of the $^5D_0$ transitions can be determined experimentally according to the following relation[25]

$$\frac{A_R}{A_{md}} = \frac{\int I_{^5D_0}(\nu)\, d\nu}{\int I_{md}(\nu)\, d\nu} \tag{6}$$

where $\int I_{^5D_0}(\nu)\, d\nu$ and $\int I_{md}(\nu)\, d\nu$ are the integral intensities of the corresponding emission spectra. The determined $^5D_0$ radiation rates A_R for the La_2O_3/Eu^{3+} samples are listed in Table 1.

The luminescence decay curves for the La_2O_3/Eu^{3+} samples obtained by monitoring the $^5D_0 \rightarrow {}^7F_2$ transition are shown in Figure 5. The luminescence decay curves can be fitted using the single exponential equation $I(t) = e^{-t/\tau}$, and the $^5D_0$ lifetimes τ for the La_2O_3/Eu^{3+} samples are determined and listed in Table 1.

The lifetime (τ), radiation rate (A_R), and nonradiation rate (A_{NR}) are related in the equation

$$\frac{1}{\tau} = A_R + A_{NR} \tag{7}$$

The emission efficiency η is determined by[25]

$$\eta = \frac{A_R}{A_R + A_{NR}} = \tau \cdot A_R \tag{8}$$

The calculated values of the $^5D_0$ emission efficiency η for the La_2O_3/Eu^{3+} samples are listed in Table 1.

Under the same excitation conditions, the luminescence efficiency P is proportional to the integral intensities of the emission spectra. For La_2O_3/Eu^{3+} phosphor, the $^5D_0 \rightarrow {}^7F_2$ hypersensitive electric dipole transition of Eu^{3+} ions in the C_{3v} symmetry sites in the La_2O_3 host lattice is by far the strongest among the $^5D_0 \rightarrow {}^7F_J$ transitions in the emission spectra. Consequently, on the basis of eq 4, the luminescence efficiency P can be substituted by the integral intensities of $^5D_0 \rightarrow {}^7F_2$emission to determine the relative values of the CTS feeding probability $P_{CTS,D}$ for the La_2O_3/Eu^{3+} samples. The measured

integral intensities of the $^5D_0 \rightarrow {}^7F_2$ emissions and the calculated ratios of $P_{CTS,D}$ for the La_2O_3/Eu^{3+} samples are listed in Table 1.

In view of the differences in the related parameters of the La_2O_3/Eu^{3+} samples (shown in Table 1), it is apparent that when the size of La_2O_3/Eu^{3+} phosphor decreases from bulk to nanoscale, the CTS feeding probability and the ^5D emission efficiency decrease (see the ratio of $P_{CTS,D}$ and different η for S_1 and S_2), the luminescence efficiency of La_2O_3/Eu^{3+} nanophosphor would inevitably be decreased. After the surface coating of the La_2O_3/Eu^{3+} sample, the CTS feeding probability and the ^5D emission efficiency are increased (see the ratio of $P_{CTS,D}$ and different η for S_2 and S_3), and the luminescence efficiency is improved. While having been annealed at 800 °C for 1 h, the surface coating is significantly improved; the increases in the CTS feeding probability and the ^5D emission efficiency become apparent (see the ratio of $P_{CTS,D}$ and different η for S_3 and S_4), and the luminescence efficiency is progressively improved.

3.5. Generality in the Conclusions for La_2O_3/Eu^{3+} Nanophosphors. In view of the structure data presented in the related literature, it can be seen that the enlargement in local disorder is a general feature for many kinds of Eu^{3+}-doped nanophosphors that leads to the rigidity decrease of the lattice environments.[1,15] In addition, when the phosphor size decreases to the nanoscale, the atomic layer between the optical centers and the surface is thinner, and fewer atoms and fewer chemical bonds participate in the resistance to the expansion of the excited optical centers. This is another general feature for Eu^{3+}-doped nanophosphors that leads to the rigidity decrease of the lattice environments. Consequently, it can be concluded that the enlargement of the CTS coordinate offset and the decrease of the CTS feeding probability are general features for Eu^{3+}-doped nanophosphors under CT excitation. On the other hand, as has been reported in the literature, the quenching centers formed by the defects and dangling bonds in the surface decrease the ^5D emission efficiency of the excited Eu^{3+} ions. This fact does not just fit for a certain kind of Eu^{3+}-doped nanophosphor but fits for all kinds of Eu^{3+}-doped nanophosphors. Consequently, the quenching mechanisms for the optical centers in La_2O_3/Eu^{3+} nanophosphor are characterized in general. As a result, surface coating is feasible to improve the luminescence efficiency for all kinds of Eu^{3+}-doped nanophosphors under CT excitation.

4. CONCLUSIONS

The rigidity decrease of nanosized La_2O_3/Eu^{3+} phosphor leads to the decrease of the CTS feeding probability to the ^5D states of Eu^{3+} ions in the optical centers. The energy transfer from the excited Eu^{3+} ions to the quenching centers in the surface causes the decrease of the ^5D emission efficiency. These two mechanisms play key roles in the decrease of the luminescence efficiency for nanosized La_2O_3/Eu^{3+} phosphor under CT excitation. After the surface coating and the subsequent annealing process, the related parameters influencing the luminescence efficiency of La_2O_3/Eu^{3+} nanophosphor have been proven to be apparently improved. The CTS feeding probability and the ^5D emission efficiency of La_2O_3/Eu^{3+} nanophosphor are simultaneously increased. The luminescence efficiency of the 30 nm-sized La_2O_3/Eu^{3+} sample is improved to 1.5 times with surface coating and progressively improved to 2.3 times after a subsequent annealing process. In view of the general features of the quenching mechanisms for La_2O_3/Eu^{3+} nanophosphor, the surface coating method is feasible to improve the luminescence efficiency for all kinds of Eu^{3+}-doped nanophosphors under CT excitation.

AUTHOR INFORMATION

Corresponding Author
*E-mail: shang.chun.yu@163.com.

ACKNOWLEDGMENT

This work was supported by the Program for New Century Talents at the University of China (NCET-06-0337). We also thank XiaoHua Tian and Qian Cheng (School of Materials Science and Engineering, Harbin Institute of Technology) for their warm-hearted help in the experiments.

REFERENCES

(1) Qi, Z.-M.; Liu, M.; Chen, Y.-H.; Zhang, G.-B.; Xu, M.; Shi, C.-S.; Zhang, W.-P.; Yin, M.; Xie, Y.-N. *J. Phys. Chem. C* **2007**, *111*, 1945–1950.
(2) Schmechel, R.; Kennedy, M.; Seggern, H. V. *J. Appl. Phys.* **2001**, *89*, 1679–1686.
(3) Bihari, B.; Eilers, H.; Tissue, B. M. *J. Lumin.* **1997**, *75*, 1–10.
(4) Li, L.; Zhang, S.-Y. *J. Phys. Chem. B* **2006**, *110*, 21438–21443.
(5) Maestro, P.; Huguenin, D. *J. Alloys Compd.* **1995**, *225*, 520–528.
(6) Dhanaraj, J.; Geethalakshmi, M.; Jagannathan, R.; Kutty, T. R. N. *Chem. Phys. Lett.* **2004**, *387*, 23–28.
(7) Tao, Y.; Zhao, G.; Zhang, W.-P.; Xia, S.-D. *Mater. Res. Bull.* **1997**, *32*, 501–506.
(8) Liu, H.-Q.; Wang, L.-L.; Huang, W.-Q.; Peng, Z.-W. *Mater. Lett.* **2007**, *61*, 1968–1970.
(9) Flachsbart, H.; Stöber, W. *J. Colloid Interface Sci.* **1969**, *30*, 568–573.
(10) Lin, C. K.; Kong, D. Y.; Liu, X. M.; Wang, H.; Yu, M.; Lin., J. *Inorg. Chem.* **2007**, *46*, 2674–2681.
(11) Sun, J.-Y.; Du, H.-Y.; Hu, W.-X. *Solid Luminescent Materials*; Chemical Industry Press: Beijing, 2003; Chapter 3.
(12) Dorenbos, P. *J. Phys.: Condens. Matter* **2003**, *15*, 8417–8434.
(13) Sun, J. Y.; Du, H. Y.; Hu, W. X., *Solid Luminescent Materials*; Chemical Industry Press: Beijing, 2003; Chapter 14.
(14) Sun, J. Y.; Du, H. Y.; Hu, W. X., *Solid Luminescent Materials*; Chemical Industry Press: Beijing, 2003; Chapter 5.
(15) Qi, Z.-M.; Shi, C.-S.; Zhang, W.-W.; Zhang, W.-P.; Hu, T.-D. *Appl. Phys. Lett.* **2002**, *81*, 2857–2859.
(16) Boyer, J.-C.; Vetrone, F.; Capobianco, J.-A.; Speghini, A.; Bettinelli, M. *J. Phys. Chem. B* **2004**, *108*, 20137–20143.
(17) Wang, Z.-C. *Thermodynamics and Statistical Physics*; Higher Education Press: Beijing, 2003; Chapter 7.
(18) Schmechel, R.; Winkler, H.; Li, X.-M; Kennedy, M.; Kolbe, M.; Benker, A.; Winterer, M.; Fischer, R. A.; Hahn, H.; von Seggern, H. *Scr. Mater.* **2001**, *44*, 1213–1217.
(19) Dhanaraj, J.; Jagannathan, R.; T. R. N. Kutty, T. R. N.; Lu, C.-H. *J. Phys. Chem. B* **2001**, *105*, 11098–11105.
(20) Song, H.-W.; Wang, J.-W.; Chen, B.-J.; Peng, H.-S.; Lu, S.-Z. *Chem. Phys. Lett.* **2003**, *376*, 1–5.
(21) Hirai, T.; Asada, Y.; Kamasawa, I. J. *J. Colloid Interface Sci.* **2004**, *276*, 339–345.
(22) Wang, H.; Yu, M.; Lin, C.-K.; Liu, X.-M.; Lin, J. *J. Phys. Chem. C* **2007**, *111*, 11223–11230.
(23) Ghosh, P.; Patra, A. *J. Phys. Chem. C* **2007**, *111*, 7004–7010.
(24) Lv, Q.; Li, A.-H.; Guo, F. Y.; Sun, L.; Zhao, L.-C. *Nanotechnology* **2008**, *19*, 205704/1–205704/8.
(25) Tian, Y.; Qi, X.-H.; Wu, X.-W.; Hua, R.-N.; Chen, B.-J. *J. Phys. Chem. C* **2009**, *113*, 10767–10772.
(26) Reisfeld, R.; Greenberg, E.; Brown, R. N.; Drexhage, M. G.; Jorgensen, C. K. *Chem. Phys. Lett.* **1983**, *95*, 91–94.